This document is a preprint of: C. Collmann, A. Nimr, M. Tascioglu Yalcinkaya et al., “6G Test Platform: Real-Time Transmission with a Flexible Transceiver,” in Proceedings of 2026 IEEE 5th International Symposium on Joint Communications & Sensing (JC&S 2026), Ponte di Legno, Italy, (p. 3), Jan 2026.

6G Test Platform: Real-Time Transmission with a Flexible Transceiver

Carl Collmann*, Ahmad Nimr*, Merve Tascioglu Yalcinkaya†, Gerhard Fettweis*
*Vodafone Chair Mobile Communications Systems, Technische Universität Dresden, Germany
†Barkhausen Institut, Dresden, Germany
carl.collmann@tu-dresden.de

***Abstract*—Future wireless sixth-generation (6G) communication standards demand experimental analysis of diverse use cases. Frequency bands at FR3 and FR2 pose a serious challenge in regards of synchronization and calibration of hardware components in testbeds. Previous works have introduced the concept of a flexible transceiver system as a dynamic test platform for 6G use cases and measurements. A key aspect of this system is the flexibility in regards of software and hardware aspects. The system is designed for allowing dynamic transmission parameter adjustment during run-time to enable evaluation of 6G use cases. This work outlines two use cases of the developed 6G test platform. The first focuses on real-time video streaming at FR3 ($10\,\mathrm{GHz}$) with carrier aggregation in a 4×4 multiple-input multiple-output (MIMO) configuration. The second shows joint communication and sensing at FR2 ($26\,\mathrm{GHz}$), with angle of departure (AoD) estimation. The maximum angular resolution is 8° and typical error vector magnitude (EVM) in the considered configuration is -15 to $-20\,\mathrm{dB}$.**

***Index Terms*—software-defined radio, butler matrix, 6G, multiple-input multiple-output, radio frequency transceiver**

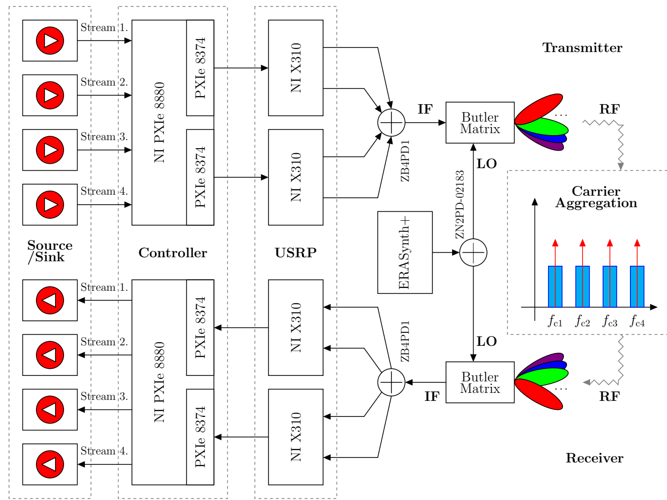

Fig. 1. Schematic of the demonstrator featuring the flexible transceiver system used for video streaming at FR2 with carrier aggregation.

I. Introduction

Future sixth-generation (6G) mobile communication networks face a diverse set of use cases that require increasingly higher data rates. Large antenna arrays in multiple-input multiple-output (MIMO) systems however introduce challenges in calibration and synchronization [1]. Furthermore, wireless networks will evolve beyond data transmission and sense the environment to allow for enhanced situational awareness [2]. Parameter estimates obtained in joint communication and sensing (JC&S) can be used for localization but also precise calibration of large antenna arrays [3]. This calibration principle using MIMO radar is explored in [4].

In order to meet the requirements of 6G applications, transceiver systems should provide flexibility of transmission parameters and be capable of adaption in real-time [5]. Key enablers in providing the desired flexibility are software-defined radio (SDR) platforms which offer programmable and reconfigurable infrastructure for experimental verification beyond the limitations of static testbeds. Related works such as [6] scan small sub-bands with their MIMO radar to highlight the feasibility of sub-Nyquist sampling.

This paper details implementation aspects of a previously described [5] flexible transceiver system which allows for dynamic RF parameter adjustment. The objective of the proposed proof-of-concept platform is to provide a scalable and dynamically reconfigurable testbed that enables real-time 6G use cases. In the demonstrator, the system is used for real-time video streaming at FR2 ($26\,\mathrm{GHz}$) and supports multi-band operation, dynamic waveform adaption and carrier aggregation (CA). Previous demonstrators using the flexible transceiver [7] operated at sub-6 GHz and were used to show angle estimation in true-time delay (TTD) systems. The 6G test platforms potential for flexible, context-aware and high performance transmissions is demonstrated, highlighting its suitability for evaluation of real-time JC&S applications.

II. System Setup

The setup of the flexible transceiver system is outlined in Fig. 1/Fig. 2 and system parameters are detailed in Table I. Key components are four universal software radio peripheral (USRP) X310, which form a 4×4 MIMO intermediate frequency (IF) transceiver. Each USRP integrates a field programmable gate array (FPGA) with DAC/ADC interfacing, optional baseband processing, and provides two independently reconfigurable RF transmit and receive chains with up to 160 MHz bandwidth and center frequencies up to 6 GHz. The USRPs are managed via an NI PXIe-1082 chassis with an embedded PXIe-8133 controller, which interfaces with the devices over PCIe and runs LabVIEW host code for configuration and IQ streaming for TX and RX. The RF frontend supports sub-6 GHz, mmWave, and sub-THz antennas,

This document is a preprint of: C. Collmann, A. Nimr, M. Tascioglu Yalcinkaya et al., “6G Test Platform: Real-Time Transmission with a Flexible Transceiver,” in Proceedings of 2026 IEEE 5th International Symposium on Joint Communications & Sensing (JC&S 2026), Ponte di Legno, Italy, (p. 3), Jan 2026.

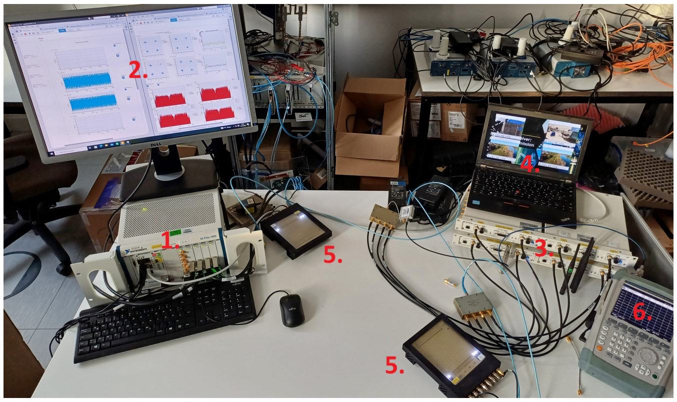

Fig. 2. Demonstrator setup in lab, 1. `NI PXIe 8880` controller, 2. TX/RX control in `NI LabVIEW`, left: TX waveform/IQ samples, right: RX constellation, spectrum and EVM, 3. `NI USRP X310` for TX/RX with GFDM modem [8], 4. video streaming laptop, 5. 16×16 Butler matrix for TX/RX at 26 GHz [9], 6. spectrum monitoring with `R&S FSH4`.

TABLE I
SYSTEM PARAMETERS.

Parameter	Symbol	Value
IF frequency	f_{IF}	2.4 GHz
LO frequency	f_{LO}	11.8 GHz
Carrier frequency	f_c	26 GHz
Bandwidth	B	20 MHz
Carrier spacing	Δf	$\{0, 10, 30, 230\}$MHz
Waveforms		OFDM, DFT-S-ODFM
Modulation		$\{4, 16, 64\}$ QAM
Configuration		4 sub-band CA

enabling flexible MIMO and carrier aggregation setups, including beamforming, combiners, and antenna arrays. The host (data source/sink) communicates with the controller through the API, orchestrates the transceiver, and streams/receives IQ samples for processing and analysis.

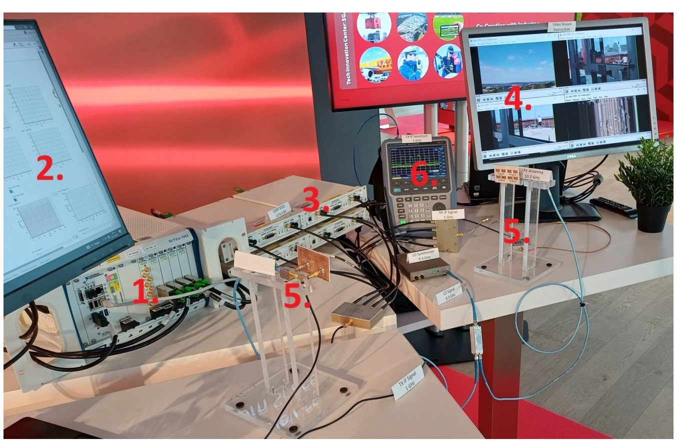

Fig. 3. FR3 video streaming demo, same components as Fig. 2.

III. DEMONSTRATION USE CASES

A. Real-Time Video transmission over FR3

This demo shows video streaming with CA at 10 GHz. The components of the demo shown in Fig. 3 are identical to Fig. 2. In the configuration of this demonstrator, a wideband antenna operating at FR3 is used. The antenna, as illustrated in Fig. 4, features a fixed beamformer with half-power beamwidth (HPBW) of $\approx 60°$. The antenna is resonant at 10.3 GHz, has a return loss of -18.7 dB, isolation of 28 dB, gain of 10.2 dBi, radiation efficiency of 97 % and VSWR of 1.28.

B. Joint Communication and sensing at FR2 using a frequency division array

In this demonstrator, a Butler matrix is used to transmit at 26 GHz (FR2 frequency band), highlighting the flexibility of the test platform. The Butler matrix [9] features 16 orthogonal beams that can be used for TX/RX, as illustrated in Fig. 6. While the Butler matrix is designed for 28 GHz, the authors in [9] also show that it can be used at different frequencies, specifically at 26 GHz [10]. The Butler matrix contains quasi-Yagi antennas, a frequency doubler for the local oscillator (LO) signal, a mixer for converting the IF signal up to the desired transmission frequency (see Table I) and amplifiers.

IV. EVALUATION AND RESULTS

In the configuration shown in this demonstrator, each of the sub-bands is assigned one of the center beams shown in Fig. 6 of the TX Butler matrix. On the RX side, the CA signal from the two center beams of the Butler matrix is fed to all RF chains. Since each sub-band has their own beam assigned, the system is called *Frequency Division Array*, which is more fitting than the more widely known term MIMO radar. Estimating the angle of departure (AoD) then is possible by estimating the RX power of each sub-band, which corresponds to the power of the TX beam assigned for the respective sub-bands. By estimating the TX beam with the maximum power, the AoD is implicitly estimated, as each beam corresponds to a certain spacial direction. The spacing of the beams then provides a coarse spatial resolution, which is $\approx 8°$ as can be seen in Fig. 6. Since the demonstrator does not contain an inertial measurement unit (IMU) as AoD reference, no explicit angle estimate is provided currently, but only the highest power beam.

The EVM is highly dependent on TX power, LO power, RX gain and distance between TX/RX. In the given configuration of $L_{\text{TX}} = -20$ dBm, $L_{\text{LO}} = 4$ dBm and a distance of $d = 1$ m the typical EVM is ≈ -18 dB, as can be seen in Fig. 5. While the EVM as shown in Fig. 5 is stable across time, sudden jumps are visible at certain time increments. These result from a burst-transmission of the frames, where sometimes at the RX only parts of the frame are detected and sometimes noise is misinterpreted as signal by the modem running on the USRP FPGA [8], which consequently cause a drop in the EVM. Fig. 7 shows the received constellation at typical EVM values for the four RF chains, with the ideal symbols marked in red. The modem [8] also supports bit error rate (BER) for

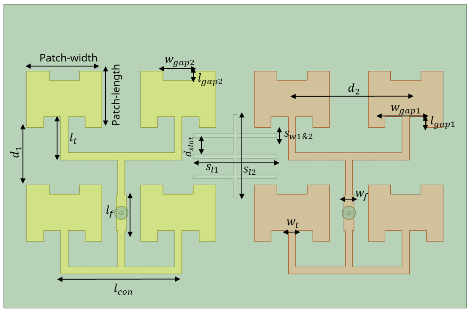

Fig. 4. 10 GHz FR3 wideband array antenna.

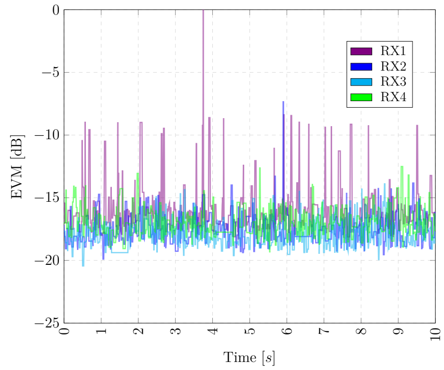

Fig. 5. EVM for 4 receive RF chains, 1000 observations with 10 ms spacing.

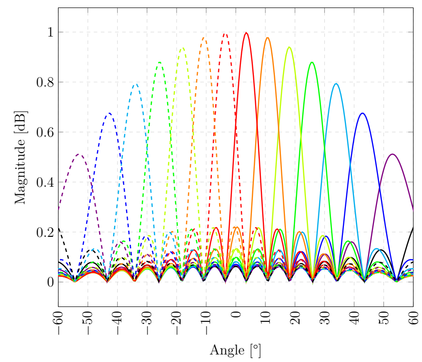

Fig. 6. 26 GHz Butler matrix response with 16 beams [9], [10].

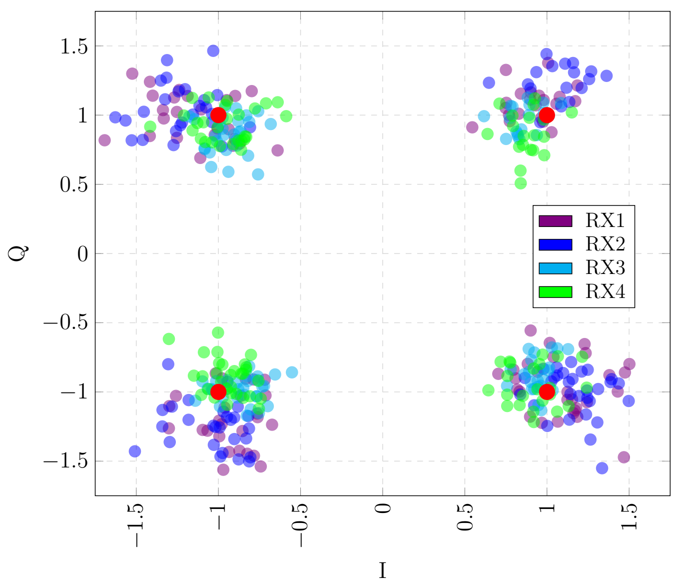

Fig. 7. IQ diagram for 4 RF chains, 100 received symbols, EVM $\in [-15, -18]$ dB, using the 4-QAM modulation of the GFDM modem [8].

the decoded symbols, however this feature is not used in this demonstrator.

V. Conclusion

This work demonstrates the capabilities of a flexible transceiver system for real-time 6G use cases. The platform provides dynamic reconfiguration of RF parameters and support for 4×4 MIMO with carrier aggregation, enabling high-performance transmissions at both FR3 (10 GHz) and FR2 (26 GHz), as well as obtaining coarse angle estimation. The system allows real-time adjustment of waveforms and transmission parameters. The demonstrator highlights the potential of flexible 6G testbeds for evaluating next-generation wireless applications. These results underscore the suitability of software-defined, dynamically reconfigurable platforms for experimentation in 6G scenarios.

Acknowledgment

This work was supported by BMFTR under the project KOMSENS-6G (16KISK124).

References

[1] H. Liu, X. Yuan, and Y.-J. A. Zhang, “Matrix-calibration-based cascaded channel estimation for reconfigurable intelligent surface assisted multiuser mimo,” *IEEE Journal on Selected Areas in Communications*, vol. 38, no. 11, pp. 2621–2636, 2020.

[2] F. Liu, Y. Cui, C. Masouros, J. Xu, T. X. Han, Y. C. Eldar, and S. Buzzi, “Integrated sensing and communications: Toward dual-functional wireless networks for 6g and beyond,” *IEEE Journal on Selected Areas in Communications*, vol. 40, no. 6, pp. 1728–1767, 2022.

[3] R. Rogalin, O. Y. Bursalioglu, H. Papadopoulos, G. Caire, A. F. Molisch, A. Michaloliakos, V. Balan, and K. Psounis, “Scalable synchronization and reciprocity calibration for distributed multiuser mimo,” *IEEE Transactions on Wireless Communications*, vol. 13, no. 4, pp. 1815–1831, 2014.

[4] V. Wirth, J. Braeunig, D. Khouri, F. Gutsche, M. Vossiek, T. Weyrich, and M. Stamminger, “Automatic spatial calibration of near-field mimo radar with respect to optical depth sensors,” in *2024 IEEE/RSJ International Conference on Intelligent Robots and Systems (IROS)*, 2024, pp. 8322–8329.

[5] B. Banerjee, C. Collmann, A. Nimr, and G. Fettweis, “Flexible transceiver platform for holistic radio design analysis,” in *6GNet 2024*, Paris, France, Oct 2024.

[6] K. V. Mishra, E. Shoshan, M. Namer, M. Meltsin, D. Cohen, R. Madmoni, S. Dror, R. Ifraimov, and Y. C. Eldar, “Cognitive sub-nyquist hardware prototype of a collocated mimo radar,” in *2016 4th International Workshop on Compressed Sensing Theory and its Applications to Radar, Sonar and Remote Sensing (CoSeRa)*, 2016, pp. 56–60.

[7] C. Collmann, A. Nimr, and G. Fettweis, “Reliable angle estimation in true-time-delay systems with real-time phase calibration,” in *2025 IEEE 5th International Symposium on Joint Communications & Sensing (JC&S)*, Oulu, Finland, Jan 2025, p. 2.

[8] Z. Li, A. Nimr, and G. Fettweis, “Implementation and performance measurement of flexible radix-2 gfdm modem,” in *2019 IEEE 2nd 5G World Forum (5GWF)*, 2019, pp. 130–134.

[9] X. Wang, M. Laabs, D. Plettemeier, K. Kosaka, and Y. Matsunaga, “28 ghz multi-beam antenna array based on wideband high-dimension 16x16 butler matrix,” in *2019 13th European Conference on Antennas and Propagation (EuCAP)*, 2019, pp. 1–4.

[10] M. K. Marandi, “Adaptive and robust beam selection in millimeter-wave massive mimo systems,” Ph.D. dissertation, TU Dresden, 2023. [Online]. Available: https://nbn-resolving.org/urn:nbn:de:bsz:14-qucosa2-858183